Eur. Phys. J. B **9**, 149–157 (1999)

THE EUROPEAN PHYSICAL JOURNAL B

EDP Sciences

Surface dependence of the magnetic configurations of the ordered B2 FeCr alloy

F. Amalou[1], M. Benakki[1], A. Mokrani[2], and C. Demangeat[3,a]

[1] Institut de Physique, Université Mouloud Mammeri, 15000 Tizi-ouzou, Algeria
[2] LPME, EA1153 DS4, 2, Rue de la Houssinière, 44072 Nantes, France
[3] IPCMS-GEMME, 23, rue du Loess, F-67037 Strasbourg Cedex, France

Received 23 March 1998

Abstract. Tight-binding linear muffin tin orbitals calculations with generalized gradient approximation were carried out for the magnetic configurations at the surface of the ferromagnetic ordered B2 FeCr alloys. For both (001) and (111) crystallographic phases, non ferromagnetic configurations are shown to be more stable than the ferromagnetic configuration of the bulk alloy. For (001) surface we display a $c(2 \times 2)$ ground state for either Cr or Fe at the surface. For Cr top layer the magnetic moments are 700% larger than in the bulk B2 FeCr while they are slightly enhanced for Fe top layer. For (111) surface an antiferromagnetic coupling between surface and subsurface is always obtained *i.e.* for either Fe or Cr at the surface. This change of coupling between Fe and Cr (from ferromagnetic to antiferromagnetic) is expected to be fundamental to any explanation of the experimental results obtained for the interface alloying at the Fe/Cr interfaces.

PACS. 75.30.Pd Surface magnetism – 75.10.Lp Band and itinerant models – 75.50.Bb Fe and its alloys

1 Introduction

The angular resolved Auger spectroscopy (ARAES) [1–3], the scanning tunneling microscopy (STM) [4] and proton induced Auger electron spectroscopy [5] have shown that the formation of the Fe/Cr (001) interface is far more complicated than expected. The above studies revealed very clearly that the Cr undergoes interfaces mixing when the substrate temperature is adjusted for optimum growth. However, the quantitative conclusions based on the STM technique differ significantly from those based on Auger spectroscopy [6].

Pizzagalli *et al.* [7] have shown that contradictory experimental data on magnetic moments and spin-order at Fe/Cr interfaces can be explained by structural irregularities at the interfaces. The spin polarized electronic charge distribution was calculated by using a self consistent tight-binding model combined with a real space recursion method. It was used to interpret the total magnetic moment of Cr (001) films and of Cr/Fe (001) sandwiches MBE grown on Fe (001) from in situ measurements with an alternating gradient magnetometer during film growth. With the same model as Pizzagalli *et al.*; Bouzar *et al.* [8] have investigated the magnetic reconstruction at the surface of B2 FeCr alloy.

Uzdin and Demangeat [9] have studied within periodic Anderson model (PAM) the distribution of magnetic moments in Fe/Cr/Fe sandwiches with pinhole defects. The distribution of the moments inside the pinhole is similar to the Fe clusters embedded into a Cr matrix [10]. Uzdin *et al.* [11] have explained recent results of Cr overlayers on Fe surface by means of magnetic linear dichroism in the angular distribution and spin-resolved core level photoemission within the framework of periodic Anderson model. Comparison of experimental spectra and theoretical dependencies, obtained for the different surface roughness, leads to conclusions about the microscopic structure of Cr overlayers.

Kulikov and Demangeat [12] have performed self-consistent calculations of the spin polarized electronic structure of disordered FeCr alloy. The moments coupling is a function of the alloy concentration and for iron-rich alloys this coupling changes from parallel (ferromagnetic) to antiparallel (antiferromagnetic). It is therefore obvious that, in order to explain the magnetic profiles at the Fe/Cr interfaces it is necessary to consider both coupling between Fe and Cr *i.e.* ferromagnetic as in the B2 (FeCr) alloy [13–15] whereas for Fe_nCr_m superlattices for $n > 1$ the coupling is believed to be of antiferromagnetic type [16–18].

Up to now, calculations concerning Fe_nCr_m superlattices for $n > 1$ have been numerous and the conclusion reached is that the coupling between Fe and Cr is antiparallel (or antiferromagnetic). Recently, Moraïtis *et al.* [19] have shown within a tight-binding linear muffin tin

[a] e-mail: claude@belenus.u-strasbg.fr

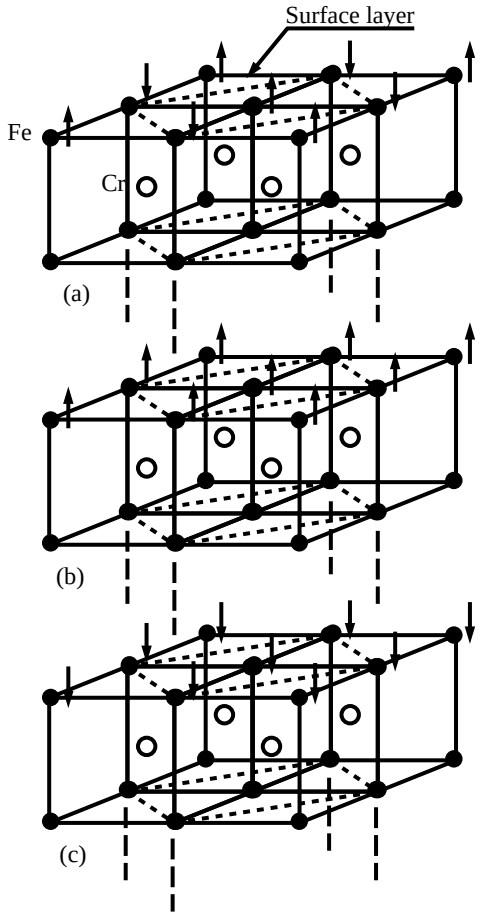

Fig. 1. Schematic view of three magnetic configurations at the surface of B2 FeCr with Fe (dark circles) at the surface: (a) c(2×2), (b) p$(1\times1)\uparrow$ and (c) p$(1\times1)\downarrow$. In dashed lines we have represented the unit cell which is used to reproduce the semi-infinite environment for all these configurations.

orbitals (TB-LMTO) approach in local density approximation (LDA), that for the B2 FeCr alloy, a slight increase of the lattice parameter leads to a change of the interfacial coupling between Fe and Cr. It may be worthwhile to remember that this alloy may be viewed as alternating (001) layers of Fe and Cr, thus forming the low thickness limit in the Fe_nCr_m multilayer family (FeCr is Fe_nCr_m superlattice for $n = 1$ and $m = 1$). It is therefore necessary to explain why the coupling at the Fe/Cr interface in Fe_nCr_m multilayers depends on n, the number of Fe layers! We [19] have already shown that the coupling depends strongly on the lattice parameter. This point has been confirmed recently by Qiu *et al.* [15] within the augmented spherical waves (ASW) approach. This coupling between Fe and Cr depends more generally on the Fe concentration as shown in disordered FeCr alloys [12].

In the present communication we want to assert the precision of the semi-empirical calculations of Bouzar *et al.* [8] displaying a transition from ferromagnetic to antiferromagnetic coupling when one goes from bulk B2 FeCr alloy to the surface. In this article we present electronic-structure calculation of different magnetic configurations for (001) and (111) crystallographic configurations at the surface of B2 FeCr alloy. In Section 2 we present briefly the TB-LMTO calculation model applied to the surface. We will discuss more precisely two points: *i*) the effect of the number of k points on the values of the magnetic moments and on the stability of the ground state configuration, and *ii*) the effect of the thickness of the supercell *slab* on the magnetic reconstruction at the surface of the B2 FeCr alloy. Section 3 presents the results obtained for B2 FeCr bulk within generalized gradient approximation. These results are discussed and compared to previous calculations. In Section 4 we present our results concerning the different magnetic configurations converged for (001) surface. The results for the (111) surface are presented in Section 5. Finally, Section 6 is devoted to the conclusion. It will be especially shown that the self consistent procedure does not converge easily, in particular for the (011) surface so that those last results will appear in a forthcoming publication.

2 Calculation model

In this paper, we report the magnetic structure at the surface of B2 FeCr alloy, using a scalar-relativistic version of the k space tight-binding linear muffin-tin orbital method [20] in the atomic sphere approximation (TB-LMTO ASA). This method has given pertinent results in the case of one Mn monolayer on Fe(001) [21], for the relative stability of an on-top and an inverted Mn monolayer an Ag (001) [22] as well as for 3d transition metal monolayers on graphite [23]. Suitable results have been also obtained for Fe_nV_m superlattices [24] and for V_m thin films ($m = 1, 4$) on Fe (001), the magnetic moment of the V monolayer being equal to $0.7\mu_B$ whereas Handschuh and Blügel [25] within full potential linearized augmented plane waves method (FLAPW) have obtained a value of $0.6\mu_B$.

In the work of Bouzar *et al.* [8] only ferromagnetic *i.e.* p$(1\times1)\uparrow$ and p$(1\times1)\downarrow$ configurations for the surface layer were considered. Here, we include also the well-known c(2×2) magnetic configuration which has been shown to be the ground state for Mn on Fe (001) [21]. In the case of (111) surface, antiferromagnetic configurations are frustrated due to the triangular geometry. Therefore, as discussed by Krüger *et al.* [23] various magnetic configurations (if we restrict to constrained collinear solutions) should be tested. Here we restrict to the most simplest row by row (noted here p(2×1)) and displayed in Figure 1a of [23]. To be able to compare between the total energies of all these configurations we have chosen the same unit cell in real space (as shown in Fig. 1 for the (001) crystallographic surface) and also the same number of k-points in the irreducible Brillouin zone has been used. In our TB-LMTO approach, in the atomic sphere approximation, we used the general gradient approximation with the Langreth-Mehl-Hu functional [26]. The model consists of *slabs* that are superposition of alternating Fe and Cr monolayers. Atomic layers are in general separated by five layers of empty spheres. This number (five) is found to

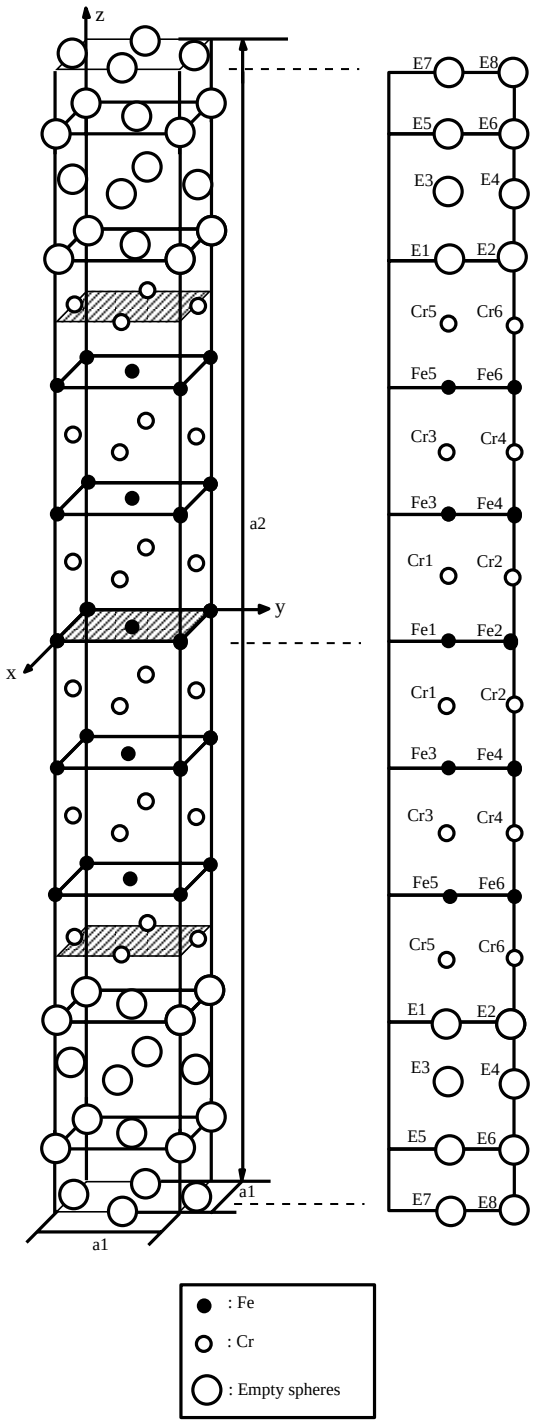

Fig. 2. Calculation model for (001) surface with Cr on top layer. This model, shown in the left side of the figure, consists of supercell slab with 11 (alternating Fe and Cr) atomic layers and 7 layers of empty spheres (Ei). In each layer we consider a pattern of two atoms that we distinguish by different indices as shown in the right side of the figure (which is a projection of the slab on the yz-plane), *i.e.* in the center of the slab we distinguish the two iron sites by Fe1 and Fe2. These atoms are inequivalent in the $c(2\times 2)$ configuration and equivalent in the $p(1\times 1)\uparrow$ and $p(1\times 1)\downarrow$ configurations. Lattice parameters are: $a_1 = \sqrt{2}\times a$ and $a_2 = 8\times a$, "a" is the lattice parameter of the B2 structure of FeCr corresponding to the ground state.

be sufficient to obtain well separated noninteracting slabs [21,22], that is charge vanishing in the central layer of empty spheres and no dispersion along the z-axis direction. However, for the specific case of B2 FeCr, we have found that five layers was not sufficient, so we will use in all the calculations seven layers in order to reach the above conditions. Empty spheres consist of pseudo atoms with no core states. They are located alternatively at the Fe and Cr sites. Their role is double: (i) reproduce the symmetry along the z-axis broken for a semi infinite system, thus allowing us to calculate electronic structure using a method operating in the k-space, (ii) break the bonds for the atoms of the top layer of the slab thus creating the surface.

We have optimized the number of k-points in order to get accurate solutions with a reasonable time of calculation. A typical set of $6\times 6\times 2$ special k-points mesh (which yield 32 points in the irreducible first Brillouin zone) is therefore used to perform Brillouin zone sampling. Also we have investigated the effect of the thickness of the slab on:
i) the stability of the magnetic surface reconstruction *i.e.* that a particular ground state should not depend on the thickness of the slab used;
ii) the values of the magnetic moments at the surface should not vary over $10^{-2}\mu_{\rm B}$.
Taking into account these two conditions we have shown that reasonable thicknesses of the slabs are 11 monolayers (ML) for (001) surface (Fig. 2) and 9 ML for (111) surface.

3 Bulk FeCr

We have computed the total energy *versus* lattice parameter for bulk B2 FeCr alloy (Fig. 3a) for Langreth-Mehl-Hu functional. The equilibrium lattice constant in bcc magnetic B2 FeCr is found to be 5.36 a.u. In Figure 3b we can see that the magnetic moments varies slowly over the entire range of lattice parameter around the ground state and shows parallel coupling between Fe and Cr magnetic moments. A transition from ferromagnetic configuration to antiferromagnetic configuration is observed for an increase of the lattice parameter by 3%. This is in qualitative agreement with the LDA results of Moraïtis *et al.* [19].

For the lattice parameter corresponding to the ground state we have obtained $1.51\mu_{\rm B}$ for Fe and $0.37\mu_{\rm B}$ for Cr. These values are different from those obtained within LMTO-LDA [14] *i.e.* $1.10\mu_{\rm B}$ and $0.68\mu_{\rm B}$ and TB-LMTO-LDA [19] *i.e.* $0.98\mu_{\rm B}$ and $0.68\mu_{\rm B}$. They are in reasonable agreement with the GGA results of Singh *i.e.* 1.21 or 1.36 for Fe depending on the lattice parameter used. It is not at all clear why GGA and LDA leads to such discrepancies. Some clues can be found in Table 1 of the paper of Moroni and Jarlborg [14] where it is shown that different results are obtained *i.e.* from 0 to $1.2\mu_{\rm B}$ for bulk Cr depending on the functional used. The Perdew-Wang functional [27] overestimates the lattice parameter of the ground state as discussed by Amalou *et al.* [28]. Moreover this functional leads to a value of $1.2\mu_{\rm B}$ for bulk Cr [14] which is twice the experimental value. Also in the case of TB-LMTO method used here with the Perdew-Wang functional a moment of

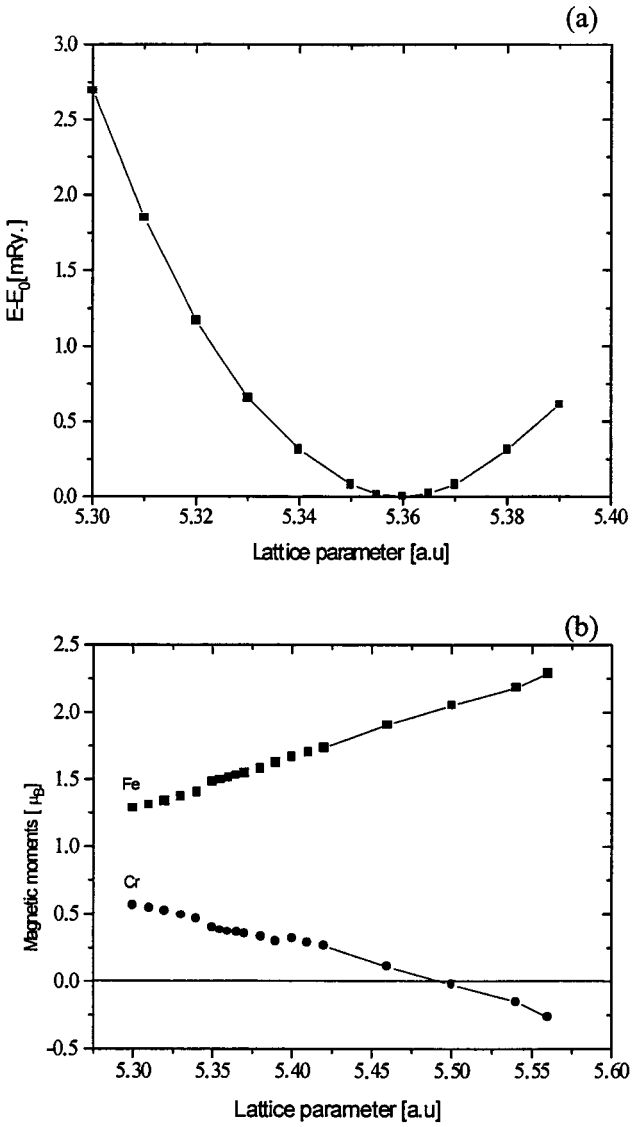

Fig. 3. Total energy (a) and magnetic moments (b) *versus* lattice parameter with Langreth-Mehl-Hu functional for Fe(squares) and Cr(circles) for B2 FeCr around the minimum of energy E_0 obtained for a lattice parameter $a_0 = 5.36$ a.u. A transition from ferromagnetic to antiferromagnetic coupling between Fe and Cr is obtained at $a_0 = 5.49$ a.u.

$1.4\mu_B$ has been obtained. On the other hand, with the Langreth-Mehl-Hu functional a moment of $0.6\mu_B$ is obtained for bulk Cr, which is in clear agreement with the experimental result. Thus in the present work, and for the particular case of B2 FeCr, we have chosen the Langreth-Mehl-Hu functional.

4 Magnetic configurations at the (001) surface

In this part we will consider two cases, namely: i) when Cr is on top layer and ii) for Fe at the surface. Calculation model for both systems is shown in Figure 2. However, to obtain well separated supercells and to reduce charge transfers in the central layers, we have been constrained to take here seven layers of empty spheres. In order to verify the validity of our model we have studied the effect of varying the number of atomic layers. We have found no fundamental effect so that relative stability of the different magnetic configurations is not altered. We have also studied the effect of increasing the number of k points in the irreducible Brillouin zone. Energies are found to be quantitatively the same: a difference $\approx 10^{-2}$ mRy/at between a set of $6 \times 6 \times 2$ and a set of $12 \times 12 \times 4$ k-points is obtained.

For Cr at the (001) surface we have obtained 3 converged solutions *i.e.* c(2×2), p$(1 \times 1)\downarrow$ and p$(1 \times 1)\uparrow$. Results are reported respectively in Figures 4a, 4b and 4c and summarized in Figures 5a, 5b, 5c. As displayed in Figure 6a, the c(2×2) antiferromagnetic configuration is shown to be the ground state. The magnetic moments of Cr are about $3\mu_B$ which is an increase of about 700% as compared to bulk B2 FeCr.

For the metastable solution p$(1\times1)\uparrow$ we recover quickly the bulk values for Fe and Cr. For the ground state *i.e.* the c(2×2) like configuration we obtain for the Cr surface values of -2.93 and 2.74 whereas for S-2 also the Cr magnetic moments are deeply modified *i.e.* the moments are 0.07 and 0.61. For p$(1 \times 1)\downarrow$ we observe an increase of the Fe magnetic moment for S-3 and S-5 whereas a strong decrease of the Cr moment is observed for S-4. Mean magnetic moment per atom is not very different from zero for Cr at the surface *i.e.* $-0.1\mu_B$ for the ground state c(2×2) configuration. This is in perfect agreement with recent "*in situ* measurements with an alternating gradient magnetometer during film growth" of Miethaner and Bayreuther [7,29,30]. In this experiment Cr layer is grown on Fe. As discussed by Heinrich [3], Davies [4] and Pfandzelter [5], alloying is formed at the surface. Therefore, if this alloy is of B2 FeCr type, then the magnetic moment at the surface is roughly zero which is the result obtained by Miethaner.

For Fe at the (001) surface we have obtained 2 converged solutions, namely c(2×2) and p$(1 \times 1)\downarrow$. As for Cr at the surface, the c(2×2) configuration is the ground state with a difference of energy of 1.7 [mRy/at] between the two configurations. A small increase of the magnetic moments of Fe is obtained. Mean magnetic moments of Fe are also not very different from zero *i.e.* in agreement with Miethaner's results [7,30] where Fe monolayers, deposited on a Cr substrate, displays a roughly zero total magnetic moment.

As summary, for both Cr or Fe at the (001) crystallographic surface of B2 FeCr the c(2×2) configuration is shown to be the ground state. These results may explain the recent results of Miethaner *et al.* [7,29,30].

5 Magnetic configurations at the (111) surface

As for the (001) surface we will consider here the two cases of Fe and Cr at the (111) surface. Since we have

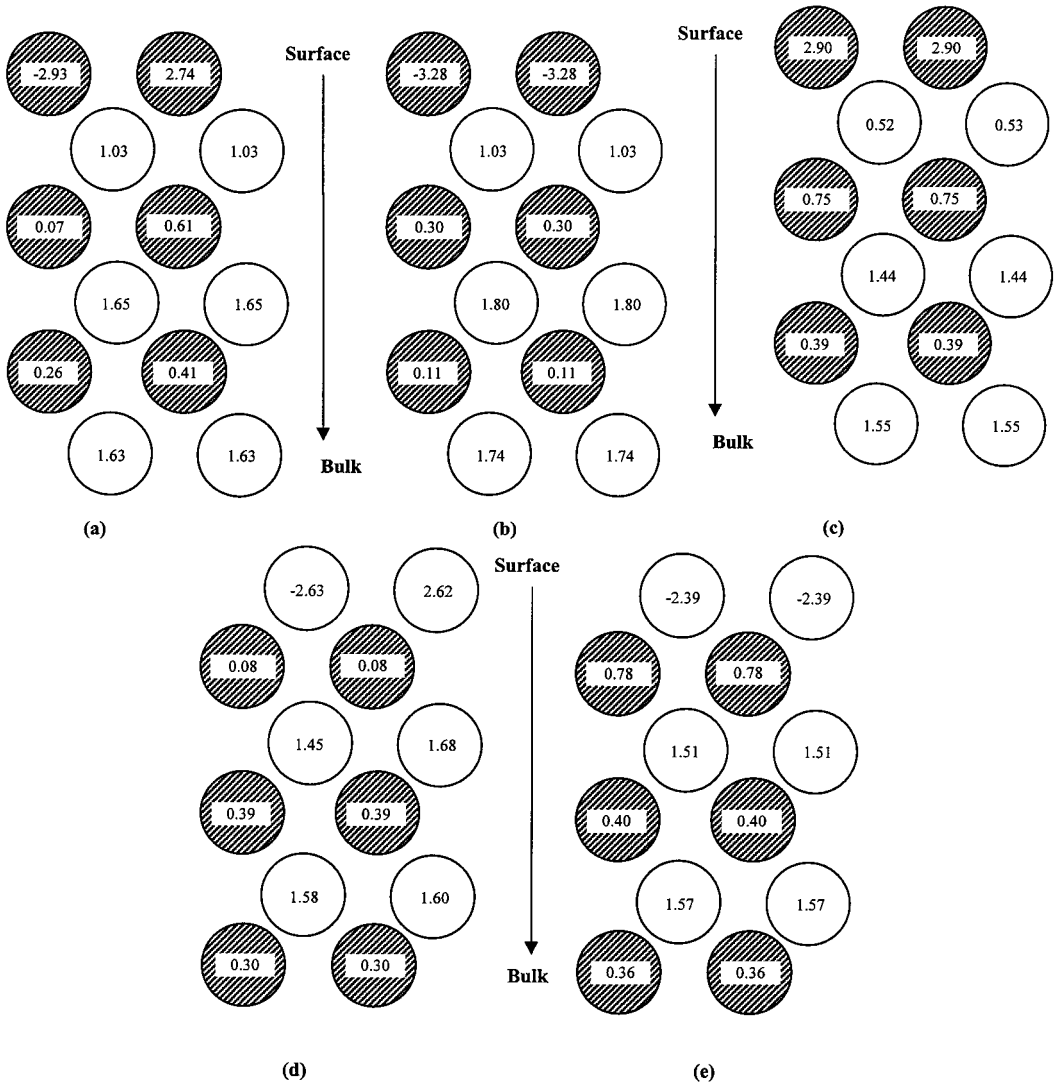

Fig. 4. Magnetic moments at the (001) FeCr surface with Cr on top layer (dark circles) in a c(2 × 2) (a), an antiferromagnetic p(1 × 1)↓ (b) and a ferromagnetic p(1 × 1)↑ (c) configuration. The case of Fe (hollow circles) on top layer is shown in a c(2 × 2) (d) and an antiferromagnetic p(1 × 1)↓ (e) configuration.

found numerical difficulties to converge the magnetic configurations on this surface, we have been constrained to reduce the number of atomic layers, so that the supercell contains in this study 9 alternating Fe and Cr layers, and 7 layers of empty spheres.

For Cr at the (111) surface we have obtained two converged solutions *i.e.* p(2×1)p(2×1)p(2×1) and p(1×1)↓. Results are shown in Figures 7a, 7b and summarized in Figures 8a, 8b. Here we have used different notations than those used for the (001) surface to indicate the long range coupling of the atomic layers. The p(2 × 1)p(2 × 1)p(2 × 1) notation indicates a p(2 × 1) antiferromagnetic coupling between the three top most layers. The p(1×1)↓ configuration is shown to be the ground state contrary to what was obtained for the (001) surface. Energy difference between the two converged configurations is about 0.7 [mRy/at]. The antiferromagnetic p(1 × 1)↓ coupling at the surface, with a mean magnetic moment of $-3\mu_{\mathrm{B}}$, can explain the results of Turtur and Bayreuther [31] if one considers that the Fe surface is highly faceted with a non negligible number of (111) domains [32].

For Fe at the (111) surface, three converged magnetic configurations are obtained: p(2×1)p(2×1), p(1×1)↓ and p(1 × 1)↑p(1 × 1)↓. As shown for Cr at the (111) surface, we have also a long range coupling. The p(2 × 1)p(2 × 1) notation indicates a p(2 × 1) antiferromagnetic coupling between the surface and the subsurface. The p(1×1)↑p(1× 1)↓ solution, obtained starting the self-consistent procedure with a ferromagnetic coupling overall the atomic layers, displays an antiferromagnetic coupling between the two top most layers. Magnetic moments are shown in Figures 7c, 7d, 7e and summarized in Figures 8c, 8d, 8e. As for Cr at the (111) surface, the p(1 × 1)↓ configuration is shown to be the ground state. Relative energies are shown in Figure 6. Mean magnetic moment at the surface layer is $-2.66\mu_{\mathrm{B}}$.

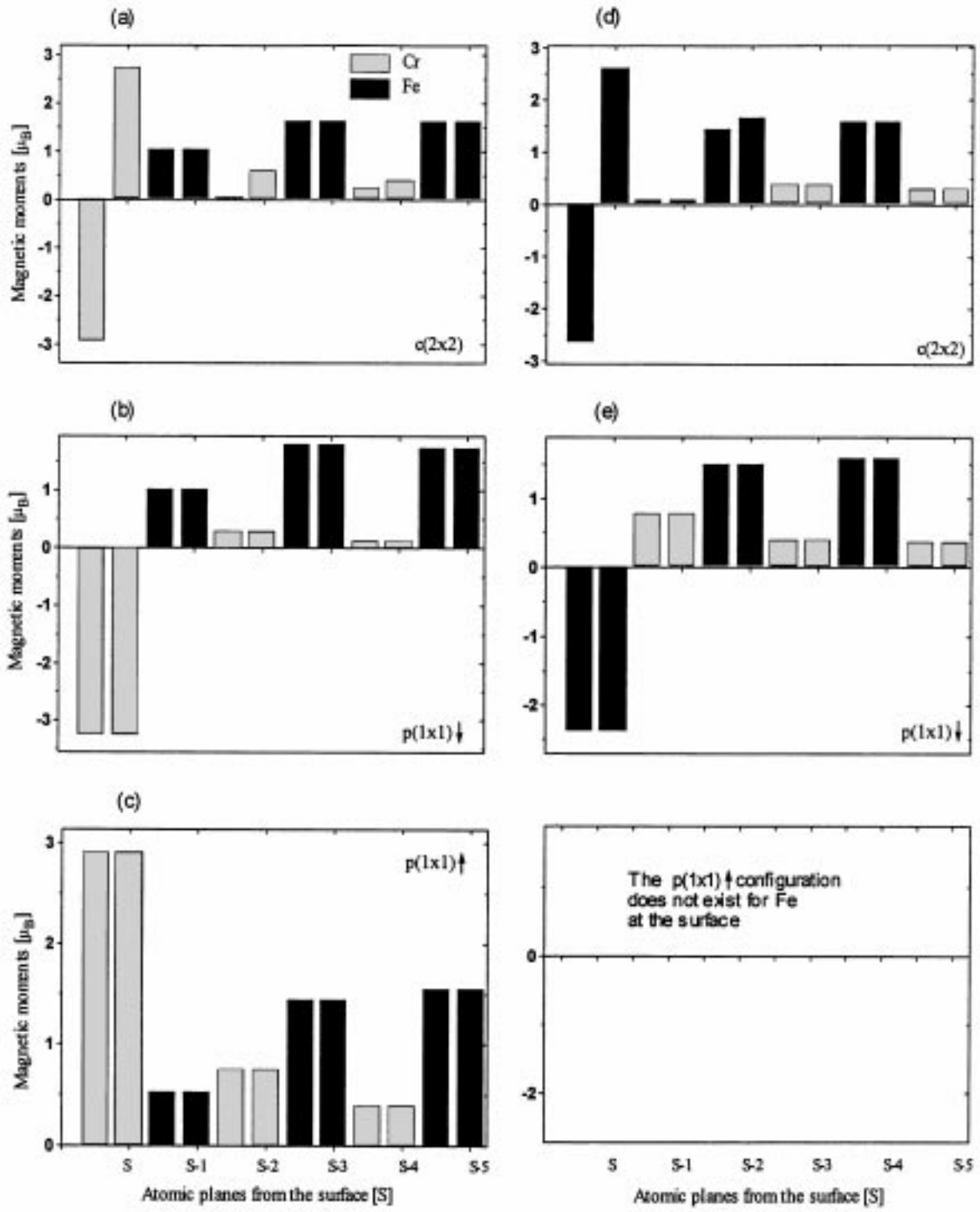

Fig. 5. Magnetic moments in the atomic layers taken from the surface [S] in the (001) crystallographic orientation. In each atomic layer we have considered two inequivalent sites represented here by the two columns in each graduation. In (a), (b) and (c) we have represented the different magnetic configurations at the surface with Cr on top layer in respectively a c(2×2), p(1×1)$\downarrow$ and p(1×1)$\uparrow$ configurations. The case of Fe on top layer is displayed in (d) and (e). We note that for Fe the p(1×1)$\uparrow$ configuration does not exist.

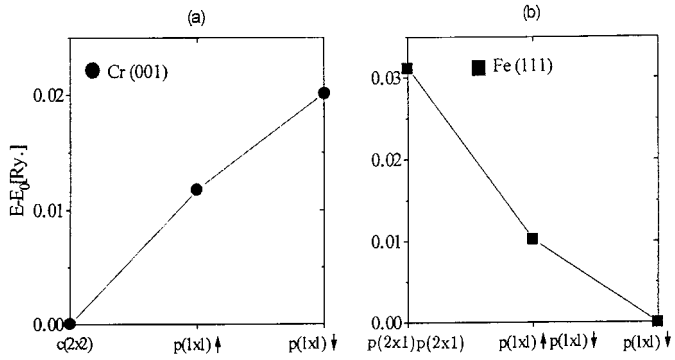

Fig. 6. Relative stability of different magnetic configurations for the (001) surface with Cr on the top layer(a) and (111) surface with Fe on the top layer (b). E_0 is the energy of the ground state.

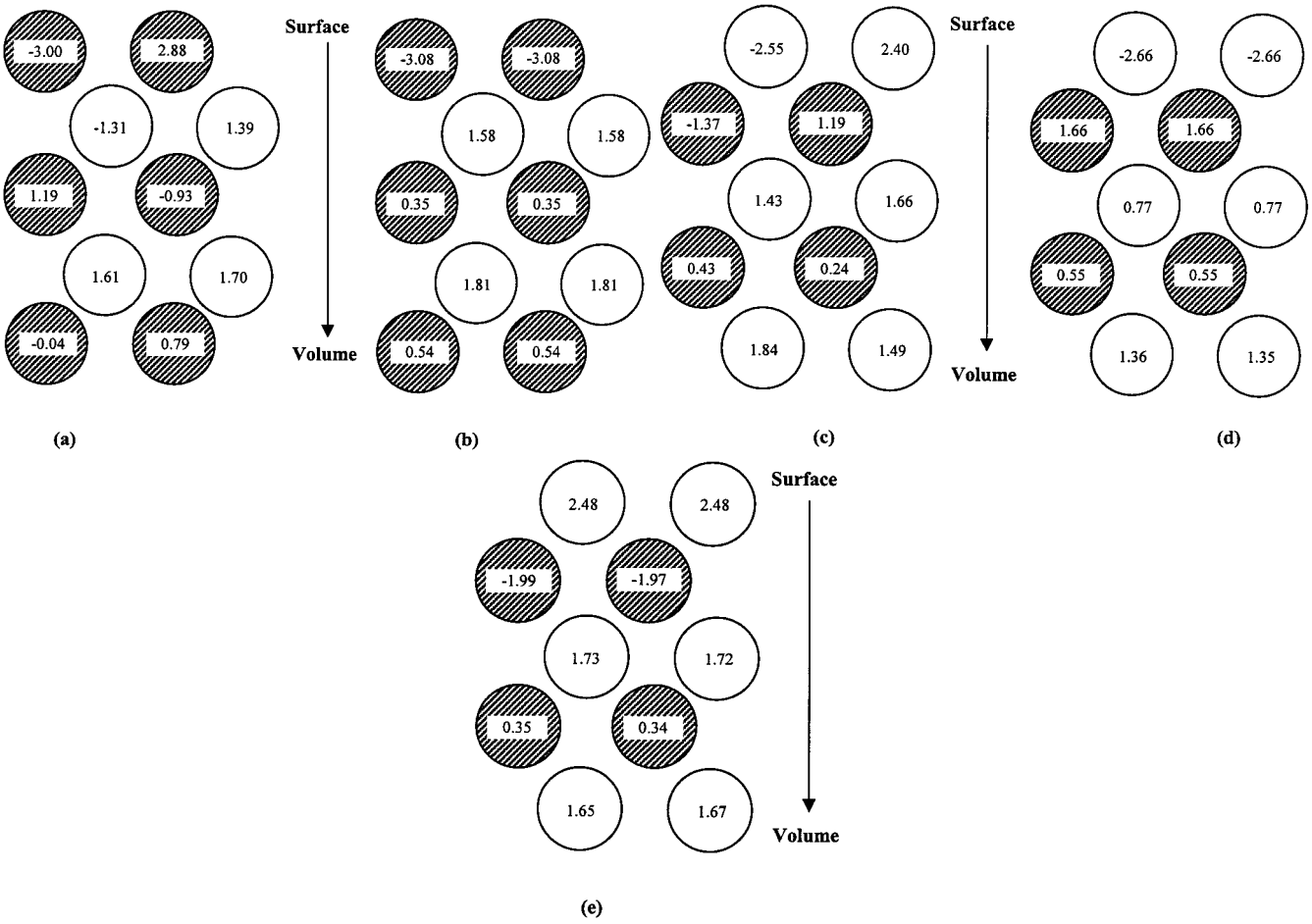

Fig. 7. Magnetic moments at the (111) FeCr surface with Cr on top layer (dark circles) in (a) a $p(2 \times 1)p(2 \times 1)p(2 \times 1)$ and (b) an antiferromagnetic $p(1 \times 1)\downarrow$ configuration. The case of Fe (hollow circles) on top layer is shown in a $p(2 \times 1)p(2 \times 1)$ (c), an antiferromagnetic $p(1 \times 1)\downarrow$ (d) and a $p(1 \times 1)\uparrow p(1 \times 1)\downarrow$ (e) configuration.

Our results show clearly the fundamental effect of the crystallographic orientation on the stability of the magnetic configurations at the surface. For the (111) surface, the magnetic moments at the surface and at the subsurface are antiferromagnetically coupled contrary to the (001) surface where the ground state is shown to be $c(2 \times 2)$. Therefore the mean magnetic moment is roughly zero for the (001) surface and about $-3\mu_B$ for (111) surface.

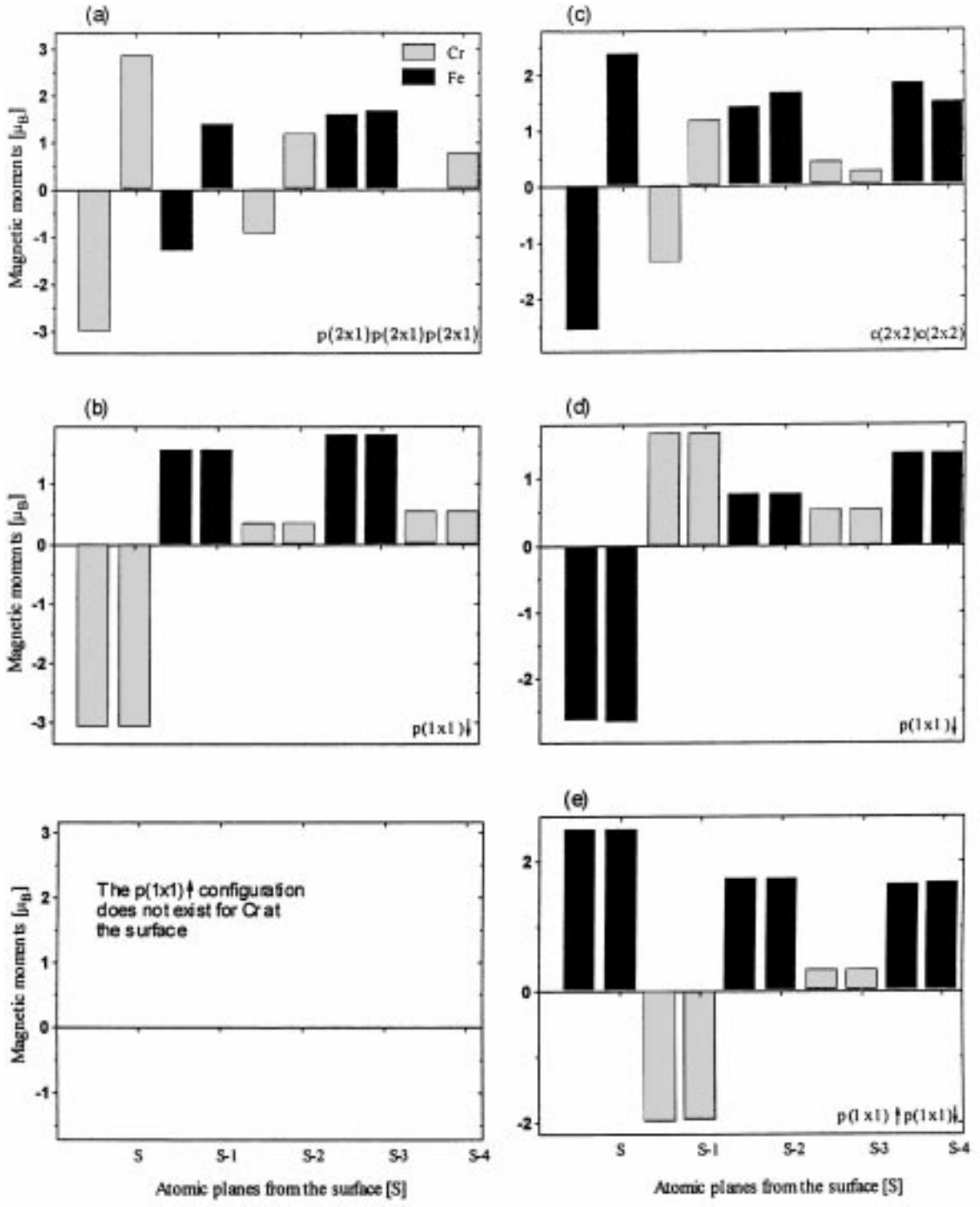

Fig. 8. Magnetic moments in the atomic layers taken from the surface [S] in the (111) crystallographic orientation. In each atomic layer we have considered two inequivalent sites represented here by the two columns in each graduation. In (a) and (b) we have represented the different magnetic configurations at the surface with Cr on top layer in respectively a $p(2\times1)p(2\times1)p(2\times1)$ and $p(1\times1)\downarrow$ configuration. For Fe at the surface, magnetic configurations are shown in (c) in $p(2\times1)p(2\times1)$ (d) $p(1\times1)\downarrow$ and (e) $p(1\times1)\uparrow p(1\times1)\downarrow$ configurations. We note that for Cr at the surface the $p(1\times1)\uparrow$ configuration does not exist.

6 Conclusion and outlook

In this communication we have displayed magnetic surface reconstruction at the B2 FeCr bulk ferromagnet. This is the first gradient corrected *ab initio* calculation on this subject. It confirms the previous semi-empirical calculations of Bouzar *et al.* [8]. The main results are: i) for the (001) surface and for Cr or Fe at the surface, a $c(2 \times 2)$ reconstruction is shown to be the ground state; ii) for the (111) surface a $p(1 \times 1)\downarrow$ magnetic configuration is shown to be the ground state.

From the experimental side [1–7,11] a convinced picture has now appeared: alloying is present at the Fe/Cr interfaces and lead to drastic changes in the interpretation of the results. It is not trivial to handle this problem theoretically because of the lack of detailed structural informations arising from experiments. Freyss *et al.* [33] have taken into account Cr diffusion into Fe substrate by considering a two-layer alloy near the Fe substrate. The rate of interdiffusion in such a model is found to play an important role when the growth mode is far from being layer by layer. However this calculation [33] was based on semi-empirical tight-binding model and the parameters used should be very sensitive to the coordination number of the Cr atom. Also, Uzdin *et al.* [11] have combined semi-empirical Periodic Anderson Model together with magnetic dichroism and spin-resolved photoemission to probe interdiffusion at the Fe/Cr interfaces. Wille *et al.* [34] have recently discussed the growth mode of Cr on Fe(001) by using Effective Cluster Interactions (ECI) which are obtained by a KKR-Green's function in the dilute limit [35]. These parameters are then used in a Monte-Carlo simulation of deposition and diffusion. These parameters are, as shown in the present communication, highly dependent on the coordination of the Cr atom. Moreover it has been shown that Fe can be not only in the usual ferromagnetic configuration but also in a $c(2\times2)$ antiferromagnetic state. It is therefore necessary, in any modelling of the growth process, to take into account not only of the isolated impurity limit [35] but also other concentrations (like the B2 FeCr). Work in this direction is in progress.

F.A. would like to thank the IPCMS-GEMME group for their kind hospitality. The Institut de Physique et Chimie des matériaux de Strasbourg is "Unité Mixte Associée au CNRS *No 7504*". This work was partly supported by the European Community Human Capital and Mobility Program trough contract *No CHRX-CT93-0369*, and by a collaborative program between France and Algeria (93MEN222).

References

1. B. Heinrich, J.F. Cochran, D. Venus, K. Totland, D. Atlan, S. Kovorkov, K. Myrtle, J. Appl. Phys. **79**, 4518 (1996).
2. D. Venus, B. Heinrich, Phys. Rev. B **53**, 1733 (1996).
3. B. Heinrich, J.F. Cochran, D. Venus, K. Totland, C. Schneider, K. Myrtle, J. Magn. Magn. Mater. **156**, 215 (1996).
4. A. Davies, J.A. Stroscio, D.T. Pierce, R.J. Celotta, Phys. Rev. Lett. **76**, 4175 (1996).
5. R. Pfandzelter, T. Igel, H. Winter, Phys. Rev. B **54**, 1 (1996).
6. B. Heinrich, J.F. Cochran, T. Monchesky, K. Myrtle, J. Appl. Phys. **81**, 4350 (1997).
7. L. Pizzagalli, M. Freyss, G. Moraïtis, D. Stoeffler, C. Demangeat, H. Dreyssé, A. Vega, S. Miethaner, G. Bayreuther, J. Appl. Phys. **81**, 4347 (1997).
8. H. Bouzar, M. Benakki, M. Zemirli, A. Mokrani, C. Demangeat, H. Dreyssé, Surf. Sci. **381**, 117 (1997).
9. V. Uzdin, C. Demangeat, J. Magn. Magn. Mater. **156**, 458 (1997).
10. M.S. Borczuch, V.M. Uzdin, J. Magn. Magn. Mater. **172**, 110 (1997).
11. V.M. Uzdin, D. Knabben, F.U. Hillebrecht, E. Kisker, Phys. Rev. B **59**, 1214 (1999).
12. N.I. Kulikov, C. Demangeat, Phys. Rev. B **55**, 3533 (1997).
13. D.J. Singh, J. Appl. Phys. **76**, 6688 (1994).
14. E.G. Moroni, T.J. Jarlborg, Phys. Rev. B **47**, 3255 (1993).
15. S.L. Qiu, P.M. Marcus, V.L. Moruzzi, Phys. Rev. **58**, 2651 (1998).
16. A. Vega *et al.*, J. Appl. Phys. **69**, 4544 (1991).
17. F. Herman, J. Sticht, M.V. Schilfgaarde, J. Appl. Phys. **69**, 4789 (1991).
18. D. Stoeffler, F. Gautier, Phys. Rev. B **44**, 10389 (1991).
19. G. Moraïtis, M.A. Khan, H. Dreyssé, C. Demangeat, J. Magn. Magn. Mater. **156**, 250 (1996).
20. O.K. Andersen, O. Jepsen, Phys. Rev. Lett. **53**, 2571 (1984).
21. O. Elmouhssine, G. Moraïtis, C. Demangeat, J.C. Parlebas, Phys. Rev. B **55**, 7410 (1997).
22. O. Elmouhssine. G. Moraïtis, J.C. Parlebas, C. Demangeat, P. Schieffer, M.C. Hanf, C. Krembel, G. Gewinner, Comp. Mat. Sci. **10**, 260 (1998).
23. P. Krüger, A. Rakotomahevitra, J.C. Parlebas, C. Demangeat, Phys. Rev. B **57**, 5276 (1998).
24. J. Izquierdo, A. Vega, O. Elmouhssine, H. Dreyssé, C. Demangeat, Philos. Mag. B **78**, 469 (1998).
25. S. Handschuh, S. Blügel, Solid. St. Comm. **10**, 633 (1998).
26. D.C. Langreth, M.J. Mehl, Phys. Rev. Lett. **47**, 446 (1981).
27. J.P. Perdew, Y. Wang, E. Engel, Phys. Rev. Lett. **66**, 508 (1991).
28. F. Amalou, H. Bouzar, M. Benakki, A. Mokrani, C. Demangeat, G. Moraïtis, Comp. Mat. Sci. 10, 273 (1998).
29. S. Miethaner, G. Bayreuther, J. Magn. Magn. Mater. **148**, 42 (1995).
30. S. Miethaner, Ph.D. thesis, Regensburg, 1998 (unpublished).
31. C. Turtur, G. Bayreuther, Phys. Rev. Lett. **72**, 1557 (1994).
32. G. Bayreuther, 1997 (private communication).
33. M. Freyss, D. Stoeffler, S. Miethaner, G. Bayreuther, H. Dreyssé, in *Current Problems in Condensed Matter*, edited by Moran-Lopez (Plenum Press, New York, 1998), p.209.
34. L.T. Wille, B. Nonas, P.H. Dederichs, H. Dreyssé, Philos. Mag. B **78**, 643 (1998).
35. B. Nonas, K. Wildberger, R. Zeller, P.H. Dederichs, Phys. Rev. Lett. **80**, 4574 (1998).